Available online at www.sciencedirect.com
SCIENCE DIRECT
Journal of Catalysis 235 (2005) 241–248
JOURNAL OF CATALYSIS
www.elsevier.com/locate/jcat

Palladium-modified catalytic membranes for the direct synthesis of H_2O_2: preparation and performance in aqueous solution

S. Melada [a,*], F. Pinna [a], G. Strukul [a], S. Perathoner [b], G. Centi [b]

[a] *Dipartimento di Chimica, University Ca' Foscari, INSTM Consortium R.U. of Venice, Dorsoduro 2137, 30123 Venice, Italy*
[b] *Dipartimento di Chimica Industriale ed Ingegneria dei Materiali, University of Messina, INSTM Consortium R.U. of Messina, Salita Sperone 31, 98166 Messina, Italy*

Received 20 May 2005; revised 20 July 2005; accepted 28 July 2005

Abstract

A series of new tubular catalytic membranes (TCMs) have been prepared and tested in the direct synthesis of H_2O_2. Such TCMs are carbon-coated asymmetric α-alumina mesoporous membranes supported on macroporous α-alumina. Pd was introduced by deposition–precipitation to obtain an even Pd particle distribution inside the membrane pore network. This type of membrane was active in the direct synthesis of H_2O_2. Catalytic tests were carried out in a semi-batch recirculating reactor under very mild conditions. Concentrations as high as 250–300 ppm H_2O_2 were commonly achieved after 6–7 h on stream, with a particularly high decomposition rate in the presence of H_2. Important features are optimization of the metal deposition procedure and preactivation. To slow down the decomposition and favor the synthesis of H_2O_2, a smooth metal particle surface is needed.

Keywords: Hydrogen peroxide; Direct synthesis; Membrane; Catalytic membrane reactor; Palladium; Heterogeneous catalysis

1. Introduction

Hydrogen peroxide is a commodity that today is almost exclusively produced by the anthraquinone process, developed in Germany in the 1930s [1]. This process is economically feasible only on large-scale plants, and the price of H_2O_2 produced is influenced by the complexity of the process and by the costly separation and concentration steps that are needed. Direct synthesis, which could be a more economic and environmentally acceptable alternative, has been known since the beginning of the 20th century [2], but no industrial application has been found, even given some successful attempts at DuPont during the 1980s [3].

Numerous patents have been filed over the past 30 years dealing with Pd metal or Pd metal alloy (e.g., Pd/X, X = Pt, Au, Ag, Ni) supported catalysts [3–9], homogeneous catalysts [10], electrochemical devices [11], and, only recently, Pd-based monoliths [12], membranes [13,14], and fast flow mixers [15,16].

Only a few related scientific works have been published in the open literature. Most of these describe the use of supported Pd or Pd alloy catalysts [17–22], colloidal Pd clusters [23–26], fuel cells [27], and Au catalysts [28,29] for the direct synthesis of hydrogen peroxide. Among these works, only one paper deals with membranes [30].

Despite the intense patent activity of major chemical companies, no successful industrial application has been claimed. This is because two severe drawbacks must be overcome for the direct synthesis: (1) the formation of explosive H_2/O_2 mixtures that should be avoided and (2) the selectivity of the reaction (whose main product is water) that is still unacceptably low. In principle, the use of specially designed catalytic membranes could overcome both problems [13,14,30].

* Corresponding author.
E-mail address: stefano.melada@unive.it (S. Melada).

0021-9517/$ – see front matter
doi:10.1016/j.jcat.2005.07.024

2. Experimental

Membranes were 10-cm-long asymmetric α-Al_2O_3 tubular supports, externally coated with a synthetic carbon layer. The carbon loading was in the range of 50–100 mg for each tube. The coating was performed by MAST Carbon Ltd., Guildford, UK, and the alumina support was supplied by Hermsdorfer Institut für Technische Keramik, Hermsdorf, Germany.

2.1. Sample preparation

Carbon-coated membranes (CAMs) were activated in CO_2 at 850 °C and then impregnated by a deposition–precipitation method (a classical method to obtain eggshell-type catalysts) optimized during this work [31–33]. This technique consisted of two steps: (1) basification of the membrane surface by soaking in a NaOH solution (0.1 mol) and (2) deposition of $Pd(OH)_2$ by precipitation from an acidic $PdCl_4^{2-}$ solution. The pH of the starting Pd(II) solution changed from 0.7 to 2.7. During impregnation, $Pd(OH)_2$ was deposited into the pore network of the external carbon layer. After Pd deposition, membranes were dried at room temperature, reduced at room temperature in H_2 flow, and washed with distilled water to remove chloride ions. Pd loading was between 1 and 2 wt% with respect to carbon loading.

2.2. Characterization

Membranes were thoroughly characterized by several techniques. Transmission electron microscopy (TEM) images were taken with a Jeol 3010, operating at 300 kV, equipped with a Gatan slow-scan CCD camera (model 794) and an Oxford Instrument EDS microanalysis detector (model 6636). External carbon layers have been scraped away with a knife to give a fine carbon powder. This was suspended in isopropyl alcohol, ultrasonicated for 5–10 min so that the particles were well dispersed and then deposited on a holey carbon film.

Scanning electron microscopy (SEM) images were taken with a Jeol JSM 5600 LV (low-vacuum) microscope. The membrane was gently broken in several chips (10–20 mm) that were subsequently attached to a support with a conductive glue and put in the microscope chamber.

N_2 physisorption isotherms were determined on small chips of the CAMs. Samples were degassed in vacuo (10^{-2} Torr) and heated at 150 °C for 2 h. N_2 physisorption isotherms were measured at −196 °C on a Micromeritics ASAP 2000 instrument. Specific surface areas were determined by the BET equation in the 0.05–0.2 p/p_0 range. Pore size distributions were calculated with the BJH method.

CO chemisorption measurements were carried out with a pulse technique on a home-made apparatus equipped with a thermostatted reactor and an ESS Genesys quadrupole mass spectrometer interfaced to a computer for data collection and analysis. CO^+ fragments ($m/z = 28$) were used for quantitative measurements. A 1/2 CO/Pd chemisorption stoichiometry was assumed for calculation [34]. Calibrations were carried out after each measurement by injecting a known amount of CO from a calibrated loop. A specially shaped sample holder was used to analyze the TCM as a whole. Because CO is strongly chemisorbed on Pd, all samples were characterized after the catalytic tests. A methanation test showed that CO is removed only above 300 °C. After the methanation step, Pd particles sintered extensively. Before each measurement, Pd was reduced in situ by passing a 5% H_2/He mixture at 25 °C, then thoroughly evacuated with He.

Pd loading was determined by atomic absorption spectroscopy (AAS) from the Pd(II) solutions used for metal deposition on the membranes. Differences between Pd concentration before and after impregnation gave the amount of loaded Pd. The reliability of this analytical method was checked as follows. Pd was extracted from membranes by soaking in boiling HNO_3. AAS determination on dissolved Pd(II) gave the loaded Pd amount. Differences of <3% were obtained by comparing the two analytical methods. Thus differential measurements on Pd solutions enabled determination of the Pd loading without destroying the membrane.

2.3. Catalytic tests

These were carried out in a semi-batch recirculation reactor (Fig. 1), with the membrane sealed in a tubular holder. From the inner side, H_2 was fed at constant pressure (2–5 bar) while an oxygen-saturated acidic solution was continuously circulated on the outer side of the membrane (where Pd was deposited) by means of a peristaltic pump (25 ml/min) equipped with special Tygon® MH tubing. The circulating solution was 100 ml of 0.03 mol H_2SO_4 containing 6 ppm of NaBr. H_2O_2 concentration was determined by permanganometric titration.

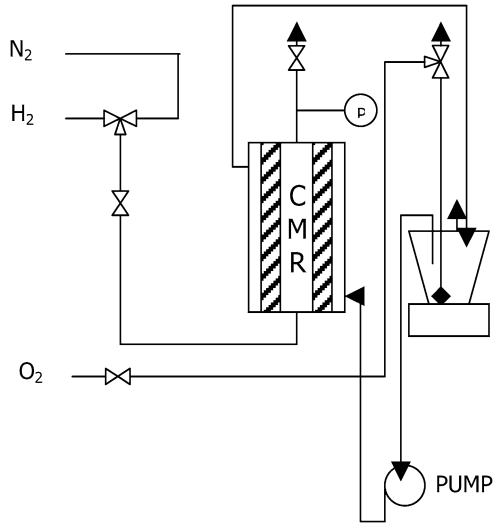

Fig. 1. Scheme of the experimental apparatus used for the catalytic tests.

3. Results and discussion

Some of the SEM images of the carbon coated asymmetric α-alumina catalytic membranes used in this work are shown in Figs. 2a–c. These images show the asymmetric structure of the membranes in details. Carbon coating does not form an external overlayer, but penetrates the mesoporous external α-alumina layer, giving rise to a microporous network inside the voids left by the Al_2O_3 particles.

The presence of both mesoporosity and microporosity is clearly demonstrated by physisorption measurements. In fact, the N_2 adsorption–desorption isotherms (two typical samples of which are given in Fig. 3) show that the nature of the carbon coating is mainly microporous, but the whole TCM exhibited a significant contribution from mesoporosity and macroporosity, reflecting the porous structure of the original Al_2O_3 particles. Consequently, a bimodal pore size distribution is observed, associated with both the microporous/mesoporous outside carbon coating structure (pore size <10 nm) and the coated macroporous alumina support skeleton (pore size >10 nm).

The starting α-alumina supports have a specific surface area of <1 m^2/g and a mean pore size of 0.3 μm (measured by mercury intrusion porosimetry), whereas the external membrane layer has a mean pore size of 100 nm. This is a consequence of the nature of the starting material, α-Al_2O_3, which is almost nonporous, so that the main pore network of the tubular support is generated by the interparticle voids. The low surface area of the starting material is then negligible with respect to the final carbon-coated TCMs' specific surface areas, so that the values obtained by BET analysis of the N_2 adsorption isotherms pertain almost exclusively to the carbon coating. The surface area of the whole TCMs ranged from 600 to about 800 m^2/g for all measured samples (see Table 1). This high surface area explains the high metal dispersion obtained with the deposition technique used in this work.

Deposition–precipitation was chosen as the preferred metal deposition method because of all the tested methods (including wet impregnation, homogeneous deposition–precipitation, and deposition–reduction), it gives the best results in term of Pd loading and reproducibility. It also has other useful features; it is simple and reliable, cheap, applicable to both inside and outside coated membranes, and, last but not least, easy to scale up.

Optimization of the deposition parameters [namely Pd(II) concentration and pH] was also carried out. pH was varied in the range 0.7–2.7 [$Pd(OH)_2$ starts precipitating at pH 3], and Pd(II) concentration was varied in the range 40–400 ppm. The procedure was carried out at room temperature. Reproducibility in metal deposition was also reflected in the reproducibility of kinetic runs; that is, samples with similar metal loading and dispersion gave very similar H_2O_2 productivity (see below).

The best compromise between Pd loading and dispersion was reached at a Pd(II) concentration of 40 ppm and a pH

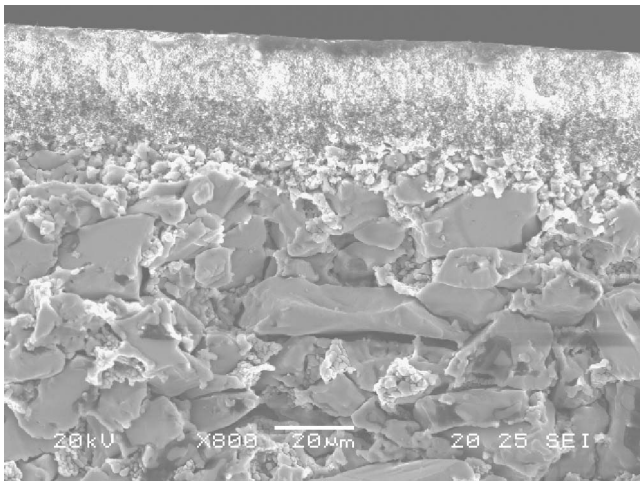

(a)

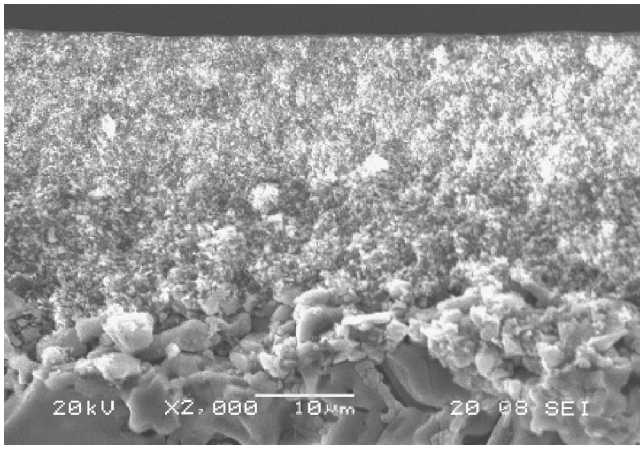

(b)

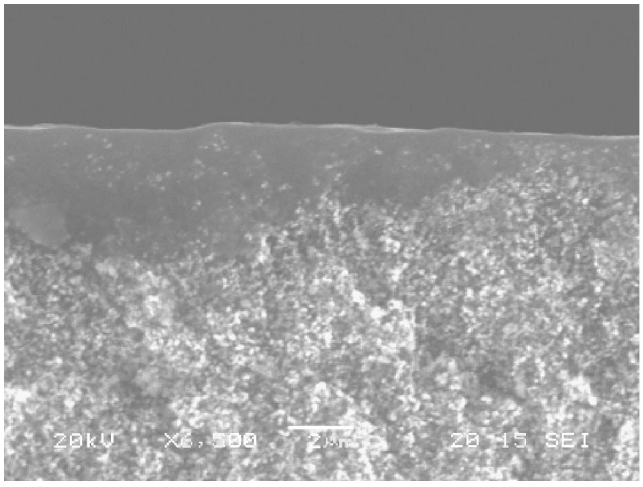

(c)

Fig. 2. SEM picture of a TCM sections (a) details of the asymmetric α-alumina meso–macroporous structure (low magnification); (b) details of the structure of the mesoporous α-alumina layers (intermediate magnification); (c) details of the presence of the carbon loading on the external α-alumina layer. The carbon layer covers the α-alumina particles giving rise to a micropores network (high magnification).

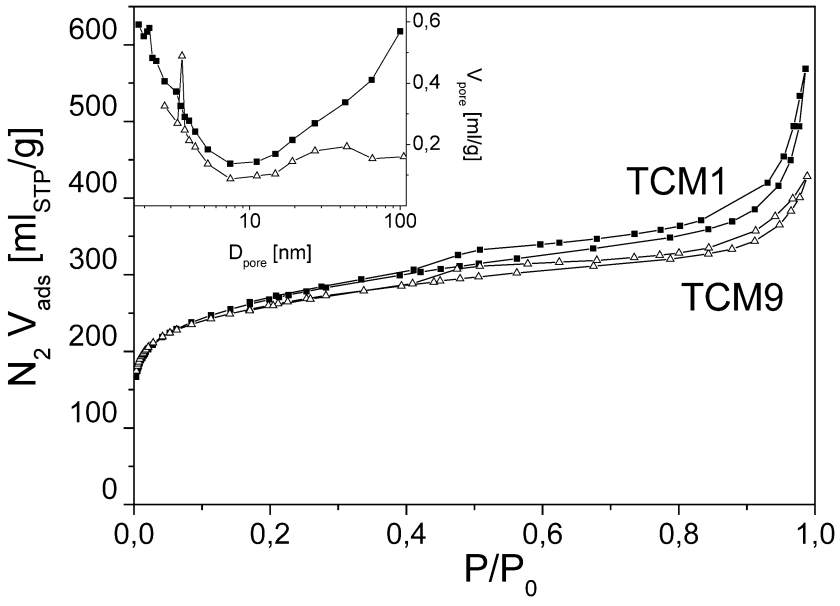

Fig. 3. N_2 adsorption isotherms and BJH pore size distributions for two chosen TCM's.

Table 1
Surface features, impregnation parameters and CO chemisorption data

Sample	BET SSA (m^2/g_{carb})	Impregnation procedure			CO chemisorption		
		Pd^{II} conc. (ppm)	Pd^{II} pH	Pd_{loaded} (mg)	A_{Pd} (m^2_{Pd}/g_{Pd})	D_{Pd} (nm)	Disp.$_{Pd}$ (%)
TCM1	748	400	1.7	4.1	15	28	4
TCM2	–			4.9	27	16	7
TCM3	584	40	2.7	1.9	16	26	4
TCM4	–		1.7	1.7	46	9.0	12
TCM5	845			1.1	26	15.5	7
TCM6	–			1.0	50	8.3	13
TCM7	634			1.0	49	8.5	13
TCM8	–		0.7	1.6	48	8.6	13
TCM9	674			0.9	65	6.4	17
TCM10	–			1.4	78	5.4	21
TCM11	636			1.1	91	4.6	24

of 0.7. Higher Pd concentrations led to the formation of an external thin Pd film that is possibly scraped away during washing and reduction steps, whereas a higher pH led to samples with lower catalytic activity. These observations are summarized in Fig. 4. The maximum Pd loading obtained by this technique was about 2 wt% with respect to the weight of the carbon coating. The optimized deposition–precipitation technique is described in the Experimental section. Surface features and impregnation results are reported in Table 1.

CO chemisorption measurements were carried out to measure the metal dispersion (see Table 1) obtained by the impregnation procedure. The effect of the Pd particle diameter on the catalytic activity can be ascertained by comparing the metal particle size of the different samples with the concentration of H_2O_2 obtained by the same samples in the catalytic experiments. As shown in Fig. 5, 8-nm Pd particles have the best catalytic performance.

Either smaller (4–5 nm) or larger (15–16 nm) Pd particles show lower overall catalytic activity. In the case of small particles, this behavior may be ascribed to the presence of highly energetic sites that can readily chemisorb O_2 dissociatively. This is supposed to be the first step in producing water [35]. In fact, atomically adsorbed oxygen could react with dissolved H_2 or H^+ to give hydroxyl species, which eventually produce water. Moreover, highly energetic sites are likely to decompose H_2O_2. Hydrogen peroxide can dissociatively chemisorb onto these sites through cleavage of the HO–OH bond. The produced surface HO species should then lead to water [36]. In the case of large particles, the low dispersion (lower number of active sites) can easily explain the low catalytic activity.

Some images showing Pd particles of small, medium, and large size are collected in Figs. 6a–c. Fig. 6a shows a small Pd particle, which is an oval-shaped monodomain Pd crystallite. About the same features were found for the 8-nm

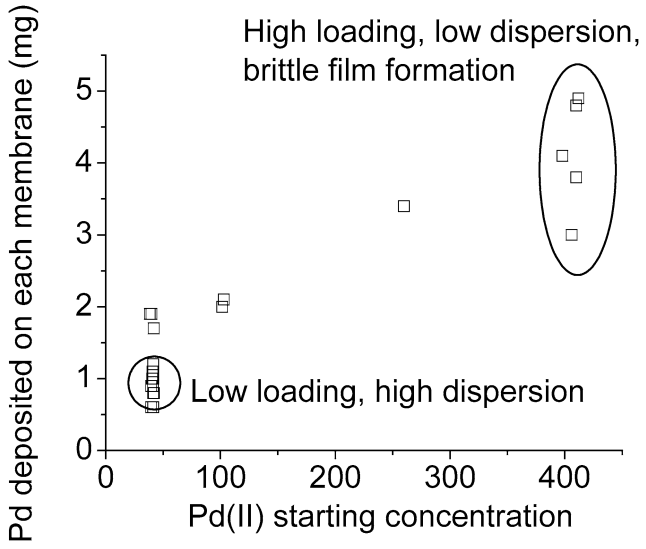

Fig. 4. Pd loading as a function of the Pd(II) concentration in the starting solution at pH 0.7.

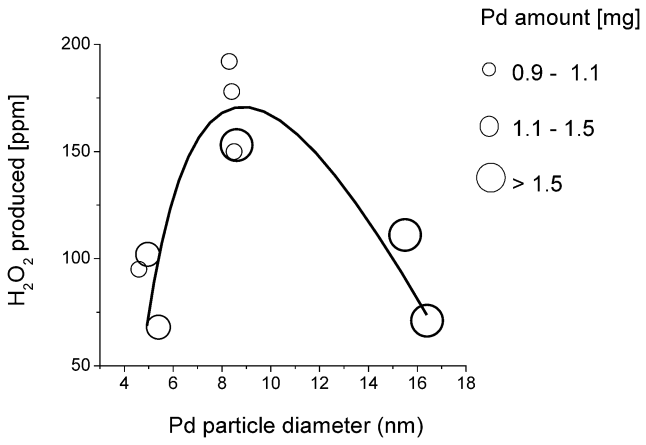

Fig. 5. Effect of the Pd particles diameter on the catalytic activity.

particles, but in this case the particle shape was more round (Fig. 6b). A large and irregular particle is shown in Fig. 6c; this is actually a cluster of small Pd crystallites with superimposed diffraction patterns.

All samples were tested for H_2O_2 synthesis in acidic aqueous solution. H_2 conversion rates are not reported because of the difficulties in measuring the actual H_2 consumption in an open system like the present one. No reliable values for H_2 mass balance could be determined.

The effect of the mean particle diameter on H_2O_2 synthesis and H_2O_2 decomposition is shown in Fig. 7. This image gives the catalytic profiles of three representative samples prepared from similar membranes but with differing particle diameters. The sample with the mean pore diameter in the optimum range (8 nm) shows the highest catalytic activity and the lowest H_2O_2 decomposition rate. Samples with Pd particles either smaller or larger than the optimum diameter have a decreased ability to synthesize H_2O_2, mainly because they have much higher decomposition rates. Thus

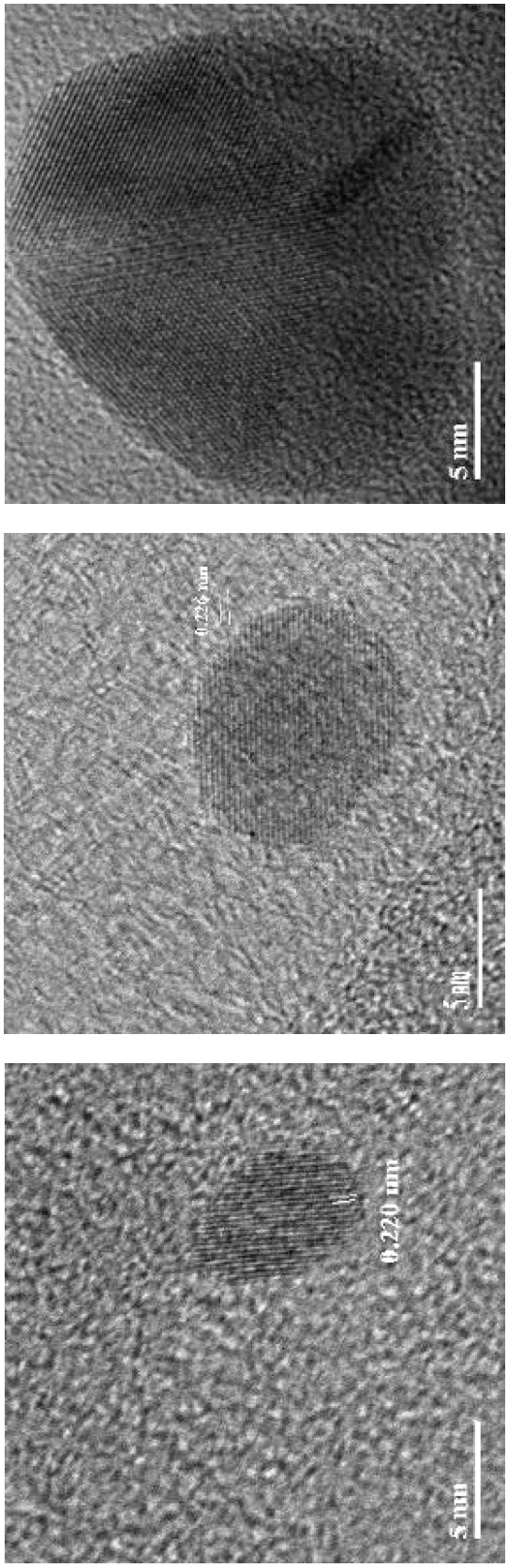

Fig. 6. TEM image of (a) small Pd particle (around 5 nm), (b) medium sized Pd particle (around 8 nm), (c) big and irregular Pd particle.

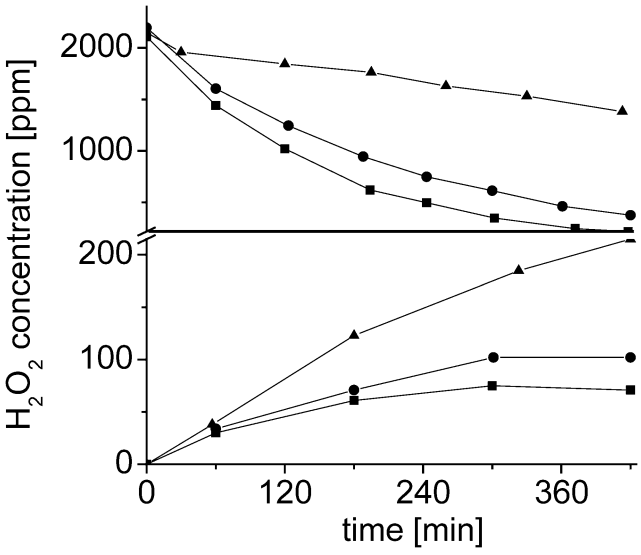

Fig. 7. Effect of the particle diameters on the catalytic performances: ▲, sample with mean particle diameter of 8 nm (TCM6); ●, 5 nm (TCM11); ■, 16 nm (TCM5).

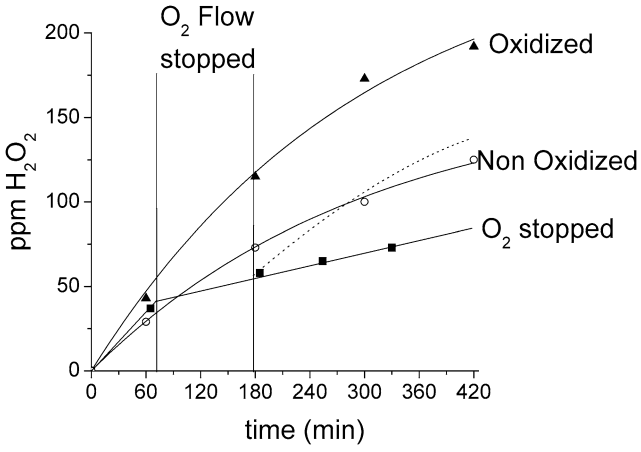

Fig. 8. Effect of the metal pre-oxidation on the catalytic activity of TCM7: ▲, pre-oxidized; ○, non-oxidized; ■, O_2 flow stopped for 2 h; dashed line, expected trend after O_2 flow restored.

the presence of highly energetic sites, found abundantly on very small and large particles, is responsible for the fast decomposition rate, which decreases the overall ability to produce H_2O_2.

An important point concerns sample pretreatment. Before kinetic tests, samples were preoxidized by flowing an O_2-saturated solution over the catalyst while at the same time replacing H_2 with an inert gas (N_2) from inside the membrane. This preoxidation step took 4 h; then the membrane was dried in N_2 flow, and a kinetic run (H_2 from inside) was carried out. The effect of the (surface) Pd oxidation state on the catalytic activity is shown in Fig. 8. Non-preoxidized samples show moderate catalytic activity (empty circles) reaching about 130 ppm H_2O_2 after 7 h on stream. With preoxidized samples (represented by the triangles in Fig. 8), catalytic activity was improved, and the final H_2O_2 concentration was as high as 200 ppm. Thus preoxidation was effective in improving the catalytic performance of the Pd particles.

This pretreatment did not lead to a bulk metal oxidation, because under the experimental conditions, only the particle surface should be covered with a monolayer of chemisorbed oxygen. This seems to be a necessary condition for improving the catalytic activity. Centi et al. [37], based on very preliminary results, stated that a reduced Pd surface was necessary for valuable catalytic activity. Indeed, the contradiction with the earlier reported results is apparent, because the active sites for H_2O_2 formation are Pd^0 centers in particles with high oxygen coverage, also making the less energetic sites available for reaction.

In a third test, the used membrane was reoxidized in the same way as before, and then a new catalytic run was started. After 1 h the oxygen stream was stopped, so that the membrane remained in contact only with H_2. As it can be seen in Fig. 8 (represented by squares), in the absence of O_2 flow there was residual catalytic activity due to the residual dissolved oxygen that led to a small increase in H_2O_2 concentration. As soon as O_2 saturation was restored, the catalytic activity was regained, but the initial H_2O_2 rate was not recovered. The expected trend is indicated by a dotted line in Fig. 8. This seems to indicate an irreversible change in the state of the Pd particles due to exposure to H_2 in the absence of O_2. If after 420 min the catalyst was surface-reoxidized following the foregoing procedure, then the initial activity was fully recovered. Reproducibility tests demonstrated that on reoxidation, the membranes could be used for several catalytic cycles without loss of activity.

In earlier work [30] we suggested a mechanism in which molecularly adsorbed O_2 on a nondefective Pd surface is responsible for H_2O_2 formation. The effect of metal particle size reported earlier in the present paper supports this view. The preoxidation effect reported herein could be interpreted in the same way, because it is reasonable that surface oxidation will be directed not only on the most energetic (defective) sites where chemisorption occurs dissociatively, but also on nondefective sites. This allows, at least initially, better production of H_2O_2. Whether or not this effect is permanent cannot be determined without selectivity data, which cannot be reliably measured in the present system.

A long-duration test was also carried out on the TCM8 sample. As can be seen from Fig. 9, the TCM was kept in the reactor for 32 h, and a maximum H_2O_2 concentration of 410 ppm was achieved after 27 h, after which the concentration began to slowly decrease. Again, after a reoxidation treatment, the catalyst could be reused several times without any significant loss of its original activity.

To study the effect of H_2 partial pressure, a diluted H_2/N_2 gas mixture was used during the kinetic tests. The results of kinetic tests with a 5% H_2/N_2 mixture are shown in Fig. 10. As can be seen, with a very dilute H_2 gas phase, only a few ppm of H_2O_2 were produced, whereas after switching to pure H_2, the catalytic activity increased to much better

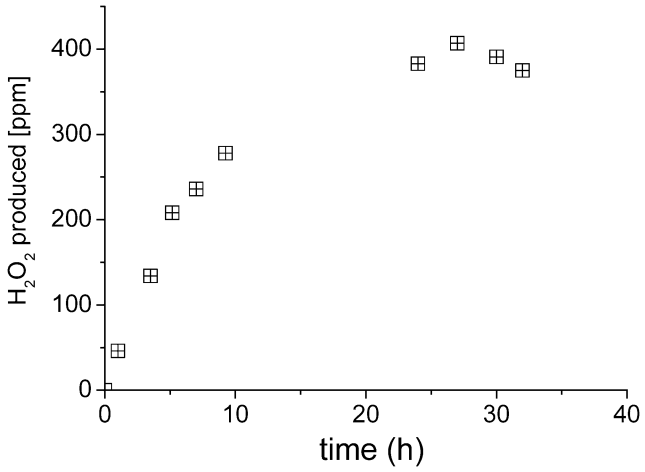

Fig. 9. Long duration test for TCM8.

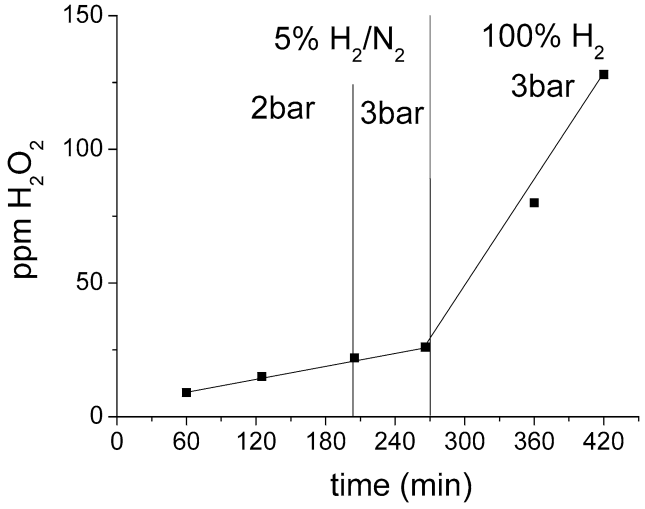

Fig. 10. Effect of the H_2 partial pressure on the catalytic activity for TCM8.

values. Fig. 10 also indicates that an increase in differential gas pressure (from 2 to 3 bar) inside the membrane was ineffective in improving catalytic performance. This means that a high H_2 partial pressure is needed for good catalytic activity toward H_2O_2 production.

Some kinetic runs were carried out by feeding pure H_2 at different total pressures. The effect of an increase in the total gas pressure inside the membrane should shift the gas–liquid interface closer to the external membrane layer until a complete blowout of the pores occurs (bubble point). According to the Young–Laplace equation, this value is theoretically several 10's of bars high, but defects in the pore structure cause it to drop (in our case, no more than 6–7 bar of differential pressure as determined experimentally, using water as the solvent). A <10% improvement in catalytic performance was observed with the TCM8 sample by increasing the internal H_2 pressure from 2 to 3 bar, and no detectable improvement was observed after further increasing the differential pressure up to 5 bar. The explored range was limited by the pore structure defects. Nonetheless, this observation provides useful information on the position of the catalytic layer, which in fact should be placed very close to the external membrane surface.

4. Conclusions

From our results, we can conclude that carbon-coated tubular ceramic membranes with palladium deposits are promising materials for the synthesis of H_2O_2 starting from hydrogen and oxygen. They are intrinsically safe, because hydrogen and oxygen are in contact only in close proximity of the palladium surface, and they can be prepared in a reliable and reproducible manner by a palladium deposition–precipitation technique. We have also demonstrated that choosing appropriate preparation parameters allows control of both metal loading and metal particle size.

Productivities up to 25–30 mmol $H_2O_2/(m^2_{TCM}\,h)$ were obtained at room temperature and under very mild conditions. Productivity is strongly dependent on metal particle size and is the result of two opposing catalytic processes, hydrogen peroxide formation and hydrogen peroxide destruction. Pd particles about 8 nm in size proved to be the best compromise, producing both better activity in hydrogen peroxide formation and lower hydrogen peroxide decomposition.

An important issue in improved H_2O_2 productivity is the existence of an oxidized Pd surface during the catalytic experiment. This is related to the mechanism through which hydrogen peroxide is formed on the Pd surface [30].

All tests were carried out at 1 bar external pressure with a few bars of inside/outside differential pressure. Under these conditions, the solubility of oxygen in water is quite modest. It is conceivable that an increase of the external oxygen pressure up to 50–60 bar significantly improves productivity, so that the system may have practical synthetic utility.

Acknowledgments

Financial support from EU (contract No. G5RD-CT2002-00678) is gratefully acknowledged. The authors are indebted to Dr. H. Richter (HITK e.V.) and Dr. S. Tennison (Mast Carbon Ltd.) for kindly providing respectively the α-alumina tubular membranes and the carbon coating.

References

[1] H.-J. Riedl, G. Pfleiderer, US Patent No. 2,215,883 (1940).
[2] H. Henkel, W. Weber, US Patent No. 1,108,752 (1914), to Henkel & Cie.
[3] L.W. Gosser, US Patent 4,681,751 (1987), to Du Pont.
[4] L. Kim, G.W. Schoenthal, US Patent No.4,007,256 (1977), to Shell Oil.
[5] Y. Izumi, H. Miyazaki, S. Kawahara, US Patent No. 4,009,252 (1977), to Tokuyama Soda.
[6] J. Van Weynbergh, J.-P. Schoebrechts, J.-C. Colery, PCT Patent No. WO92/15520 (1992), to Solvay Interox.

[7] G. Paparatto, R. D'Aloisio, G. De Alberti, R. Buzzoni, European Patent No. EP 1,160,196A1 (2001), to Eni.
[8] B. Zhou, L.-K. Lee, US Patent No. 6,168,775B1 (2001), to Hydrocarbon Technologies.
[9] B. Bertsch-Frank, I. Hemme, L. Von Hoppel, S. Katusic, J. Rollmann, US Patent No. 6,387,346B1 (2002), to Degussa-Huls.
[10] F. Moseley, P.N. Dyer, US Patent No. 4,336,240 (1982), to Air Product.
[11] J.H. White, M. Schwartz, A.F. Sammells, US Patent No. 5,645,700 (1997), to Eltron Research.
[12] F. Klemens, K. Gerd, S. Achim, F. Martin, H. Wolfgang, Q. Stefan, M. Klemens, PCT Patent No. WO98/16463 (1998), to BASF.
[13] J.A. McIntyre, S.P. Webb, PCT Patent No. WO95/30474 (1995), to Dow Chemical.
[14] V.R. Choudary, S.D. Sansare, A.G. Gaiwad, US Patent No. 6,448,199B1 (2002), to Council of Scientific & Industrial Research – India.
[15] H.A. Hutchins, US Patent No. 5,641,467 (1997), to Princeton Advanced technology Inc.
[16] K.M. Vanden Bussche, S.F. Abdo, A.R. Oroskar, US Patent No. 6,713,036 (2004), to UOP.
[17] V.V. Krishnan, A.G. Dokoutchaev, M.E. Thompson, J. Catal. 196 (2000) 366.
[18] A.G. Gaiwad, S.D. Sansare, V.R. Choudhary, J. Mol. Catal. A 181 (2002) 143.
[19] P. Landon, P.J. Collier, A.F. Carley, D. Chadwick, A.J. Papworth, A. Burrows, C.J. Kiely, G.J. Hutchings, Phys. Chem. Chem. Phys. 5 (2003) 1917.
[20] V.R. Choudhary, C. Samanta, A.G. Gaikwad, Chem. Commun. (2004) 2054.
[21] V.R. Choudhary, C. Samanta, Catal. Lett. 99 (2005) 79.
[22] R. Burch, P.R. Ellis, Appl. Catal. B 42 (2003) 203.
[23] J.H. Lunsford, J. Catal. 216 (2003) 455.
[24] S. Chinta, J.H. Lunsford, J. Catal. 225 (2004) 249.
[25] Y.-F. Han, J.H. Lunsford, J. Catal. 230 (2005) 313.
[26] Y.-F. Han, J.H. Lunsford, Catal. Lett. 99 (2005) 13.
[27] I. Yamanaka, T. Onizawa, S. Takenaka, K. Otsuka, Angew. Chem. Int. Ed. 42 (2003) 3653.
[28] M. Okumura, Y. Kitagawa, K. Yamaguchi, T. Akita, S. Tsubota, M. Haruta, Chem. Lett. 32 (2003) 822.
[29] P. Landon, P.J. Collier, A.J. Papworth, C.J. Kiely, G.J. Hutchings, Chem. Commun. (2002) 2058.
[30] V.R. Choudary, A.G. Gaiwad, S.D. Sansare, Angew. Chem. Int. Ed. 40 (2001) 1776.
[31] L.A.M. Hermans, J.W. Geus, Stud. Surf. Sci. Catal. 3 (1979) 113.
[32] A.J. van Dillen, J.W. Geus, L.A.M. Hermans, J.v.d. Meijden, in: G.C. Bond, et al. (Eds.), Proceedings of the Sixth International Congress Conference on Catalysis, London, 1976, p. 677.
[33] K.P. de Jong, Stud. Surf. Sci. Catal. 63 (1991) 19.
[34] G. Fagherazzi, P. Canton, P. Riello, N. Perticone, F. Pinna, M. Battagliarin, Langmuir 16 (2000) 4539.
[35] P. Paredes Olivera, E.M. Patrito, H. Sellers, Surf. Sci. 313 (1994) 25.
[36] S. Abate, G. Centi, S. Melada, S. Perathoner, F. Pinna, G. Strukul, Catal. Today 104 (2005) 325.
[37] G. Centi, R. Dittmeyer, S. Perathoner, M. Reif, Catal. Today 79–80 (2003) 139.